A Quaternion-Based Bang-Bang Attitude Stabilizer for Rotating Rigid Bodies[1]

Edoardo Serpelloni [2], Manfredi Maggiore [3], and Christopher J. Damaren [4]
University of Toronto, Toronto, ON, M5S 2J7, Canada.

This paper presents a quaternion-based bang-bang feedback controller solving the attitude stabilization problem for inertially symmetric spacecraft. The proposed controller is hybrid, and it relies on a hierarchical switching logic. At the high-level, a supervisor avoids unwinding by selecting between two different hybrid controllers. These low-level controllers locally stabilize a desired attitude by viewing the rigid body dynamics as a perturbation of three decoupled double-integrators. It is proved that the proposed controller locally stabilizes the desired attitude to any desired accuracy without inducing high-frequency switching in the actuators. Extensive numerical simulations suggest that the convergence of the proposed controller is global, and that the controller's performance is unaffected by small external bounded perturbations, asymmetry of the spacecraft and measurement noise.

I. Introduction

This paper presents a novel feedback controller that stabilizes the attitude of a rigid body to any degree of accuracy. Its main feature is that it is bang-bang and, as argued below, it constitutes the first solution to the attitude stabilization problem with on-off actuators and bounded switching frequency.

Although many modern spacecraft are equipped with actuators that can provide smooth torque inputs, on-off jet thrusters still play a prominent role in performing reorientation maneuvers for large spacecraft. Vehicles like the ATV [1], and the Orion spacecraft [2], rely exclusively on jet-thrusters to perform any attitude maneuver. Given the typical performance limitations affecting modern jet-thrusters, it is of crucial importance to design bang-bang controllers that do not induce high-frequency switching behaviors.

The problem of designing bang-bang attitude stabilizers has been intensively studied in the past. Most existing solutions apply to the case of small angles and planar maneuvers ([3], [4]). Approximate techniques based on the use of PWM (Pulse Width Modulation) and PWPFM (Pulse Width Pulse Frequency Modulation) have been proposed in this context, [5]. These techniques, however, introduce a problematic coupling between the switching frequency and the asymptotic bound on the state, even in the absence of external perturbations. A review of some of these techniques can be found in [6].

A robust bang-bang feedback controller was proposed in [3] for the simplified case of single-axis maneuvers. The controller is obtained by introducing dead-bands about the parabolic switching curves of the classical bang-bang time-optimal controller for double-integrators. The controller is

---

[1] This research was supported by the Natural Sciences and Engineering Research Council of Canada (NSERC).
[2] PhD Candidate, Electrical and Computer Engineering Department; edoardo.serpelloni@mail.utoronto.ca.
[3] Professor, Electrical and Computer Engineering Department; maggiore@control.utoronto.ca.
[4] Professor, University of Toronto Institute for Aerospace Studies; damaren@utias.utoronto.ca. Associate Fellow AIAA.

Published in *Journal of Guidance, Control, and Dynamics,* vol. 40, no. 6, pp. 1523–1534, 2017

robust with respect to constant uncertainties in the system's parameters and constant external torques. A bang-bang hybrid attitude stabilizer was presented by the authors of this paper in [7] for the case of planar maneuvers. The proposed controller practically stabilizes a target spacecraft orientation despite external unknown bounded perturbations and measurement noise, while keeping the number of controller's switches uniformly bounded over compact time intervals. A rigorous analysis of the controller's features can be found in [8].

Designing bang-bang controllers for general, three-dimensional maneuvers, is far more challenging. Most of the results proposed in the literature originate from various attempts to find the solution to the time-optimal attitude control problem in the case of rest-to-rest maneuvers, and result in open-loop controllers. It was shown in [9] that for an inertially symmetric spacecraft, the time-optimal controller is indeed bang-bang. It was observed through simulations that the controller induces a total of only five switches in the control input value if the reorientation maneuver is smaller than 72 deg., a total of seven switches otherwise. The control values and switching times were computed numerically, through continuation techniques. These results were later extended to asymmetric rigid spacecraft in [10], under the assumption that the control input magnitude is significantly larger that the nonlinear gyroscopic term in the dynamics. Also in this case, the control values and switching times were computed through approximate numerical procedures. The results presented in [10] confirmed the findings presented in [9]. More recently, new trajectories have been found numerically in [11] that are characterized by six control switches. In [12], the problem of performing a time-optimal reconfiguration for an axisymmetric rigid spacecraft, by using only two control torques, was tackled and solved numerically.

All the controllers discussed above require complex numerical procedures in order to generate accurate enough estimates of the optimal control input values and switching times. The very nature of the numerical schemes adopted to solve the optimization problem heavily influences the quality of the solution found. Moreover, initial guesses for states, co-states and control inputs are often required. As is to be expected, these controllers are inherently non-robust to external unmodeled perturbations, uncertainty in the system's parameters, or measurement noise.

A control strategy based on a sequence of eight bang-bang maneuvers was proposed in [13]. First, a discontinuous controller is applied to bring the spacecraft to a rest configuration, i.e., zero angular velocity. A sequence of seven single-axis bang-bang maneuvers is then performed that exploit the structure of the kinematic and dynamic equations. The authors of [13] point out that this particular control strategy suffers from a lack of robustness to both external perturbations and measurement noise, in that unmodeled perturbations may prevent the controller from successfully completing one of the maneuvers. Moreover, each single-axis bang-bang maneuver may induce sliding modes when external perturbations and measurement noise are considered. Sliding mode controllers with piecewise-constant components, as in [14], are ill-suited to be applied to solve the spacecraft attitude control problem, in that the control input switching frequency is theoretically infinite along the sliding manifold.

The problem of designing a robust feedback stabilizer that solves the bang-bang attitude control problem without inducing high-frequency switching remains, to this day, open. A controller based on the Euler angles attitude parametrization was proposed in [7] by the authors of this paper. There, it is shown that the proposed controller solves the bang-bang attitude control problem locally. In this paper the controller presented in [7] is modified so to take full advantage of the quaternion parametrization of the spacecraft attitude. The proposed controller is hybrid (each control input depends on the dynamics of a discrete variable) and hierarchical, in that a high-level supervisor switches between two distinct controllers in order to avoid the insurgence of unwinding. It is rigorously proved that the proposed controller locally solves the bang-bang attitude control problem without inducing high-frequency switching. These results are proved assuming the full nonlinear dynamics of the spacecraft. An extensive Monte Carlo numerical analysis indicates that the controller might in fact yield global practical stability. The controller's robustness with respect to measurement noise and external perturbations is also investigated through extensive simulations.

The paper is organized as follows. Section II formulates the problem investigated in this paper. Section III presents the controller solving the problem. The stability proof of the paper main results is presented in Section IV. An extensive Monte-Carlo numerical simulation is presented in Section V. The robustness of the proposed controller to measurement noise and external perturbations is investigated in Section VI and VII, respectively.

Notation: We denote $B_\epsilon(0) = \{x \in \mathbb{R}^2 : (x^\top x)^{1/2} < \epsilon\}$ and $\bar{B}_\epsilon(0) = \{x \in \mathbb{R}^2 : (x^\top x)^{1/2} \leq \epsilon\}$. These definitions imply that the set $B_0(0)$ is empty, while $\bar{B}_0(0) = \{0\}$. The 3×3 identity matrix is denoted by I. Throughout the paper, sets are denoted by capital letters. The boundary of a set A is defined as $\partial A = \bar{A} \setminus \text{Int}A$ where $\bar{A}$ is the closure of A and Int$A$ is its interior. We denote by $-A$ the set $-A = \{x : -x \in A\}$.

II. Model and Problem Formulation

Consider an inertially symmetric rigid spacecraft. Let $\mathcal{I}$ be an inertial frame, and attach a frame $\mathcal{B}$ to the center of mass of the spacecraft in such a way that the frame axes coincide with the principal axes of the spacecraft. With this convention, the inertia tensor of the spacecraft has the form $J = J_0 I$, where J_0 is a positive scalar. Let $\Omega \in \mathbb{R}^3$ denote the angular velocity of the spacecraft expressed in body frame. The spacecraft attitude is uniquely described by a rotation matrix $R \in SO(3)$, where $SO(3)$ is the set of 3×3 orthogonal matrices with unitary determinant,

$$SO(3) = \{R \in \mathbb{R}^{3\times 3} : R^\top R = RR^\top = I, \det R = +1\}.$$

For any $x \in \mathbb{R}^3$, let $S(x)$ be the skew-symmetric matrix defined as

$$S(x) = \begin{bmatrix} 0 & -x_3 & x_2 \\ x_3 & 0 & -x_1 \\ -x_2 & x_1 & 0 \end{bmatrix}$$

such that, for any $v \in \mathbb{R}^3$, $x \times v = S(x)v$. The rotational dynamics of the spacecraft is modeled by the set of equations

$$\begin{aligned} \dot{R} &= RS(\Omega) \\ J_0\dot{\Omega} &= \tau, \end{aligned} \tag{1}$$

with state $(R, \Omega) \in SO(3) \times \mathbb{R}^3$. It is assumed that the on-board actuators can deliver a bang-bang torque about each axis of the spacecraft, i.e., $\tau_i \in \{-\bar{\tau}_i, 0, +\bar{\tau}_i\}$, with $\bar{\tau}_i > 0$, $i = 1, 2, 3$.

The goal is to design a bang-bang feedback controller that practically stabilizes an equilibrium $(R^\star, 0)$, with $R^\star \in SO(3)$. In this context, the adverb "practically" signifies "approximate stabilization to any desired degree of accuracy". In other words, the goal is to design a controller able to asymptotically stabilize any arbitrarily small neighborhood U of $(R^\star, 0)$. It is assumed, without loss of generality, that $(R^\star, 0) = (I, 0)$. To comply with modern jet-thrusters performance limitations, another requirement for the control design is that the controller must never generate sliding modes or high-frequency switching behaviors.

To simplify the control design, the quaternion parametrization of spacecraft orientation is used. Consider the 3-dimensional sphere $\mathbb{S}^3 = \{x \in \mathbb{R}^4 : x^\top x = 1\}$. Any element of $SO(3)$ can be parametrized by a unit quaternion $q = (\epsilon,\ \eta) \in \mathbb{S}^3$ using the Rodrigues formula, [15], $r : \mathbb{S}^3 \to SO(3)$, $r(q) = I + 2\eta S(\epsilon) + 2S(\epsilon)^2$. In what follows, the north pole of the 3−sphere is denoted by $\mathbb{1} := (0, 1)$. Using the quaternion representation, system (1) can be rewritten as follows

$$\begin{aligned} \dot{\epsilon} &= \tfrac{1}{2}\left(\eta I + S(\epsilon)\right)\Omega \\ \dot{\eta} &= -\tfrac{1}{2}\epsilon^T\Omega \\ \dot{\Omega} &= u, \end{aligned} \tag{2}$$

with state $\chi = (q, \Omega) \in X$, where $X = \mathbb{S}^3 \times \mathbb{R}^3$ denotes the state space of system (2). Each control acceleration u_i is given by $u_i \in \{-\bar{u}_i, 0, +\bar{u}_i\}$, where $\bar{u}_i = \tau_i/J_0$. The major advantage

afforded by working with the quaternion parametrization lies in the reduction of the number of parameters used to describe the spacecraft attitude. This choice, however, comes at a price: it is a well known fact that $r : \mathbb{S}^3 \to SO(3)$ is a two-to-one mapping, i.e., if $R = r(q)$, then $R = r(-q)$ as well. In particular, both the north pole $\mathbb{1}$ and south pole $-\mathbb{1}$ of $\mathbb{S}^3$, map to the rotation matrix I, and therefore two distinct equilibria $(q, \Omega) = (\mathbb{1}, 0)$ and $(q, \Omega) = (-\mathbb{1}, 0)$ in (2) correspond to the equilibrium $(R, \Omega) = (I, 0)$ for system (1). This causes the well-known unwinding behavior when the control design is carried out without taking this fact into proper consideration. As argued in [16], to avoid unwinding in a neighborhood of the target equilibria it is necessary and sufficient to simultaneously stabilize both equilibria $(q, \Omega) = (\mathbb{1}, 0)$ and $(q, \Omega) = (-\mathbb{1}, 0)$ of system (2).

A precise statement of the problem investigated in this paper is given below.

Bang-Bang Attitude Control Problem: Consider system (2) and the desired attitude $P = \{(q, \Omega) \in X : q = \pm\mathbb{1},\ \Omega = 0\}$. Design a bang-bang feedback controller $\tau = (\tau_1, \tau_2, \tau_3)$ with $\tau_i \in \{-\bar{\tau}_i, 0, +\bar{\tau}_i\}$, $i = 1, 2, 3$, such that

i) The set P is *practically stable* for the closed-loop system. In other words, given an arbitrarily small neighborhood U of P in X, there exist controller parameters and a compact set W, with $P \subset \text{Int}W \subset U$, such that W is asymptotically stable for the closed-loop system.

ii) The number of controller switches is *uniformly bounded* over compact sets of initial conditions and over compact time intervals: for any compact set $W_0 \subset X$ and for any $T > 0$, there exists $N \in \mathbb{N}$ such that for any $(q(0), \Omega(0)) \in W_0$ the controller switches value at most N times over any time interval of length T.

In other words, we seek to design a feedback bang-bang controller able to steer the state of system (2) inside an arbitrarily small neighborhood of the target configuration in finite time, without inducing high-frequency switching in the actuators.

III. Main Results

We propose to solve the bang-bang attitude control problem by designing a hybrid controller that relies on a hierarchical switching logic. The control architecture, depicted in Figure 1, is comprised of two hierarchical layers. At the high level, a supervisor automaton $\mathcal{H}(\delta)$ (where δ is a user-defined parameter) is responsible for preventing unwinding and broadcasts an output value $h \in \{-1, 1\}$ to the low level. At the low level, three automata $\mathcal{A}_i(p_i, h)$, $i = 1, 2, 3$ (p_i is a vector of user-defined parameters) are driven by the supervisor through the parameter $h \in \{-1, 1\}$, and are responsible for the assignment of the control values u_i, $i = 1, 2, 3$.

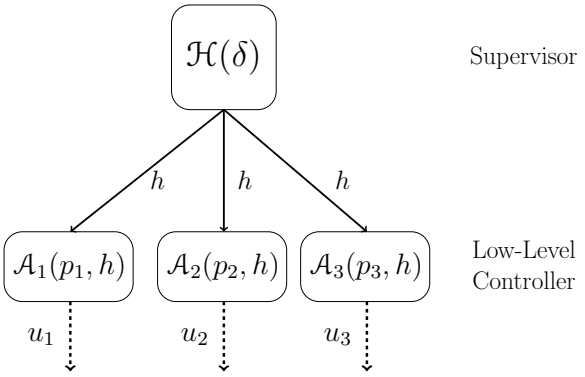

Fig. 1: Pictorial representation of the proposed control structure.

The high-level automaton $\mathcal{H}(\delta)$ selects which equilibrium to stabilize between $(q, \Omega) = (\mathbb{1}, 0)$ and $(q, \Omega) = (-\mathbb{1}, 0)$. It does so by implementing a hysteresis mechanism as in [15], the result of

which is the numerical value of parameter $h \in \{-1, +1\}$. Each low-level automaton $\mathcal{A}_i(p_i, h)$ assigns the control input $u_i \in \{-\bar{u}_i, 0, +\bar{u}_i\}$ so as to stabilize (ϵ_i, Ω_i) to a neighborhood of $(0, 0)$ whose size depends on the parameters in p_i, and to stabilize η to a neighborhood of $h = \pm 1$, which is decided by the supervisor.

A. Supervisor: Automaton $\mathcal{H}(\delta)$

The supervisor $\mathcal{H}(\delta)$ is depicted below.

$\mathcal{H}(\delta)$

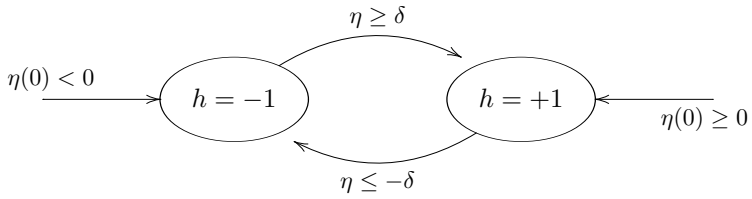

(3)

Referring to Figure 1, the automaton above monitors the scalar part of the quaternion, η, and it chooses the desired value of η to be stabilized, $+1$ or -1, through the choice of the parameter h. The idea is quite simple. If $\eta \geq \delta > 0$, then the supervisor assigns $h = +1$, while if $\eta \leq -\delta < 0$, it assigns $h = -1$. If $\eta \in (-\delta, +\delta)$, h is assigned according to an hysteresis mechanism, similarly to what was done in [15], to avoid undesired switching in the presence of measurement noise. As in [15], the hysteresis mechanism presents a trade-off between robustness with respect to measurement noise and unwinding in the hysteresis region $(-\delta, +\delta)$.

B. Low-Level Controllerr: Automata $\mathcal{A}_i(p_i, h)$ and Control Assignment $u_i^\star$

The low-level controller consists of three automata $\mathcal{A}_1, \mathcal{A}_2, \mathcal{A}_3$, each driven by h, the output of the supervisor. Each automaton $\mathcal{A}_i$ monitors the variables (ϵ_i, Ω_i) and assigns the control value $u_i \in \{-\bar{u}_i, 0, +\bar{u}_i\}$ so as to drive (ϵ_i, Ω_i) to a neighborhood of $(0, 0)$. The idea for doing so is to view the (ϵ_i, Ω_i) dynamics as a perturbation of a double-integrator, and use the double-integrator stabilizer in [8] and [17]. As mentioned earlier, the supervisor output h is used to decide which equilibrium should be stabilized. Let $\xi_i = (h\epsilon_i, \omega_i)$, where h is the output of $\mathcal{H}(\delta)$ currently broadcasted to the low-level controller. The automata $\mathcal{A}_i$ are given below.

$\mathcal{A}_i(p_i, h)$

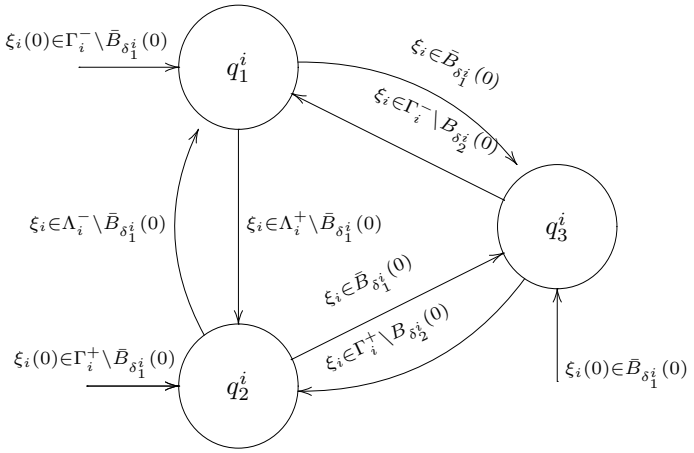

(4)

In the above, Γ_i^+, Γ_i^- are the **initialization sets** (see Figure 2) defined as

$$\begin{aligned} \Gamma_i^+ &= \{(\epsilon_i, \Omega_i) : \epsilon_i > 0,\ \Omega_i \leq -2\sqrt{\bar{u}_i \epsilon_i}\} \cup \{(\epsilon_i, \Omega_i) : \epsilon_i \leq 0,\ \Omega_i < 2\sqrt{-\bar{u}_i \epsilon_i}\}, \\ \Gamma_i^- &= -\Gamma_i^+, \end{aligned} \tag{5}$$

Λ_i^+, Λ_i^- are the **switching sets** (see Figure 3a) defined as

$$\begin{aligned} \Lambda_i^+ &= \{(\epsilon_i, \Omega_i) : \epsilon_i \leq 0,\ \Omega_i \leq 2\sqrt{-\kappa_i \bar{u}_i \epsilon_i}\} \cup \{(\epsilon_i, \Omega_i) : \epsilon_i > 0,\ \Omega_i \leq -2\sqrt{\bar{u}_i \epsilon_i}\}, \\ \Lambda_i^- &= -\Lambda_i^+, \end{aligned} \tag{6}$$

with $\kappa_i \in [0, 1)$. Letting set $Q^i = \{q_1^i, q_2^i, q_3^i\}$ denote the set of states of automaton $\mathcal{A}_i(p_i, h)$, each control input u_i is assigned through the feedback $u_i^\star : Q_i \to \mathbb{R}$ defined as

$$\begin{aligned} u_i^\star(q_1^i) &= -\bar{u}_i \\ u_i^\star(q_2^i) &= +\bar{u}_i \\ u_i^\star(q_3^i) &= 0. \end{aligned} \tag{7}$$

Notice that each feedback $u_i^\star$ depends only on the current active state of automaton $\mathcal{A}_i$, whose dynamics is driven by continuous states (ϵ_i, Ω_i).

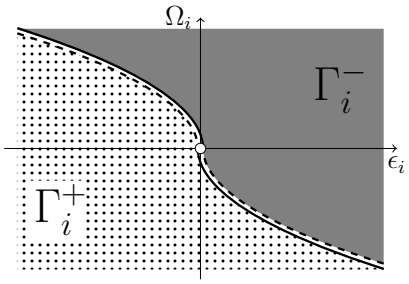

Fig. 2: Initialization sets Γ_i^+, Γ_i^-.

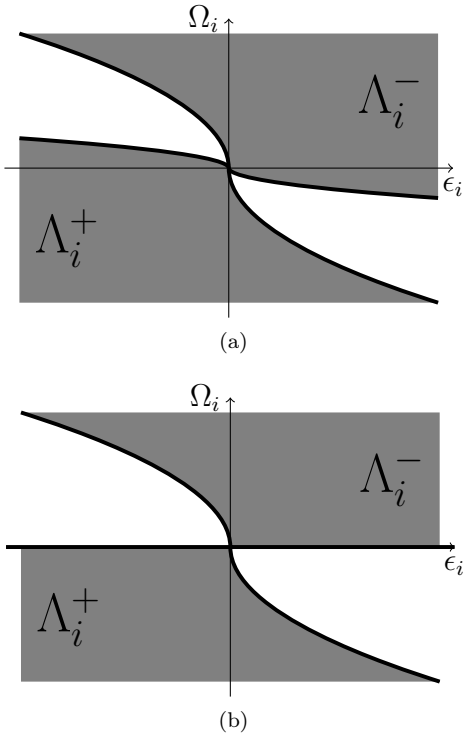

Fig. 3: Switching sets Λ_i^+, Λ_i^-, with $\kappa_i \in (0, 1)$, (a), and with $\kappa_i = 0$, (b).

In [8], it is shown that, when $\kappa_i = 0$, the automaton (4) and the feedback in (7) globally

practically stabilize the origin of the double integrator

$$\begin{aligned}\dot{\epsilon}_i &= \Omega_i,\\ \dot{\Omega}_i &= u_i^\star.\end{aligned}$$

The idea in the proof of Theorem III.1 below is to view system (2) as a perturbation of three decoupled double-integrator and exploit the stabilization property of the foregoing double-integrator stabilizer. The automaton $\mathcal{A}_i(p_i, h)$ is parametrized by the vector $p_i = (\delta_1^i, \delta_2^i, \kappa_i)$ of user-defined parameters, and by h, the output of the supervisor automaton. The parameters δ_1^i, δ_2^i determine the size of the neighborhood of $(\epsilon_i, \Omega_i) = (0, 0)$ being stabilized, while the parameter κ_i is useful for proving the theoretical stabilization properties of the attitude controller, but can be set to zero in practice. When $\kappa_1 = \kappa_2 = \kappa_3 = 0$, the switching sets are as in Figure 3b. More comments on the choice of controller parameters are provided in Section V.

The main result of the paper is stated below.

Theorem III.1 Consider system (2) where J_0 is a positive parameter and $\tau = (\tau_1, \tau_2, \tau_2)$ is restricted to have values $\tau_i \in \{-\bar{\tau}_i, 0, +\bar{\tau}_i\}$. For any $\bar{\tau}_i > 0$, $i = 1, 2, 3$, the hybrid feedback controller given by supervisor (3) and three copies of automata (4) with feedback (7) solves the bang-bang attitude control problem. In particular, the following two properties hold for the closed-loop system:

i) For any neighbourhood U of the set $P = \{(q, \Omega) \in X : q = \pm\mathbb{1}, \Omega = 0\}$, there exist controller parameters $\delta_1^i, \delta_2^i > 0$, $\kappa_i > 0$, $i = 1, 2, 3$, and $\delta \in (0, 1)$ such that U has a compact subset W containing P in its interior which is asymptotically stable.

ii) The number of controller switches is uniformly bounded in the sense stated in part (ii) of the problem statement in Section II.

IV. Proof of Theorem III.1

To simplify the analysis, it is assumed that the actuators provide the same torque about each axis, i.e., $\bar{\tau}_i = \bar{\tau}$ for all $i = 1, 2, 3$. As proposed in [9], consider a time scaling factor of $\sqrt{\bar{\tau}/J_0}$ and define the non-dimensional angular velocity as $\omega = \Omega\sqrt{J_0/\bar{\tau}}$. The spacecraft rotational dynamics in Eq. (2) can be rewritten as follows

$$\begin{aligned}\dot{\epsilon} &= \tfrac{1}{2}\left(\eta I + S(\epsilon)\right)\omega\\ \dot{\eta} &= -\tfrac{1}{2}\epsilon^T\omega\\ \dot{\omega} &= u,\end{aligned} \tag{8}$$

where $u_i = \tau_i/\bar{\tau} \in \{-1, 0, +1\}$ is the non-dimensional control input about the i-th axis. In the following, it is shown that the set $P = \{(q, \omega) \in X : q = \pm\mathbb{1}, \Omega = 0\}$ is practically stable for system (8) with controller (3), (4), (7). Since P is the union of two isolated equilibria, one needs to show that each equilibrium $(q, \Omega) = (\mathbb{1}, 0)$ and $(q, \Omega) = (-\mathbb{1}, 0)$ is practically stable. It will now be shown that $(q, \Omega) = (\mathbb{1}, 0)$ is practically stable. The proof of practical stability of the other equilibrium is identical. Consider the function $V^+ : X \to \mathbb{R}$ defined as

$$V^+(q, \omega) = V_1(\epsilon_1, \omega_1) + V_2(\epsilon_2, \omega_2) + V_3(\epsilon_3, \omega_3), \tag{9}$$

where function $V_i : \mathbb{R} \times \mathbb{R} \to \mathbb{R}_{\geq 0}$, $i = 1, 2, 3$, is given by

$$V_i(\epsilon_i, \omega_i) = 4\epsilon_i^2\omega_i\sigma(\epsilon_i, \omega_i) + \frac{4}{3}\omega_i^3\epsilon_i + \frac{3}{20}\omega_i^5\sigma(\epsilon_i, \omega_i) + \frac{4}{5}\left(2\epsilon_i\sigma(\epsilon_i, \omega_i) + \frac{1}{2}\omega_i^2\right)^{\frac{5}{2}},$$

with $\sigma : \mathbb{R} \times \mathbb{R} \to \{-1, 0, +1\}$ given by

$$\sigma(\epsilon_i, \omega_i) = \begin{cases} \operatorname{sign}\left(2\epsilon_i + \frac{1}{2}|\omega_i|\omega_i\right), & \text{if } 2\epsilon_i + \frac{1}{2}|\omega_i|\omega_i \neq 0\\ \operatorname{sign}\left(\omega_i\right), & \text{if } 2\epsilon_i + \frac{1}{2}|\omega_i|\omega_i = 0\\ 0, & \text{if } (\epsilon_i, \omega_i) = (0, 0). \end{cases}$$

The functions V_i were first proposed in [21], where it was shown that each V_i is C^1 and positive definite with respect to the origin. Hence, V^+ is C^1 and $V^+(q,\omega)=0$ if and only if $(\epsilon,\omega)=(0,0)$, so that V^+ is positive definite near the equilibrium $(q,\Omega)=(\mathbb{1},0)$. In the following, denote $\dot{V}^+$ the time-derivative of function V^+ along the solutions of the closed-loop system computed between any two consecutive state transitions of the automata. Further, we denote by $q^i \in Q^i$ the current state of automaton $\mathcal{A}_i(p_i,h)$. The following lemmas are used in the sequel.

Lemma IV.1 Consider the Lyapunov function $V^+ : X \to \mathbb{R}$ defined in Eq. (9) and let $V^+_{\epsilon_i} = \partial V^+/\partial \epsilon_i$ and $V^+_{\omega_i} = \partial V^+/\partial \omega_i$. There exist $\alpha,\beta>0$ such that the following inequality holds

$$\dot{V}^+ \leq \sum_{i=1}^{3} -\lambda_i(q,\omega_i,u_i^\star(q^i)), \tag{10}$$

where the function $(q,\omega_i) \mapsto -\lambda_i(q,\omega_i,u_i^\star(q^i))$ is continuous and defined as $-\lambda_i(q,\omega_i,u_i^\star) = 1/2V^+_{\epsilon_i}\eta\omega_i + V^+_{\omega_i}u_i^\star(q^i) + \alpha\sqrt{1-\eta^2}\epsilon_i^2 + \beta\sqrt{1-\eta^2}\omega_i^4$, and q^i is the current state of automaton $\mathcal{A}_i(p_i,h)$.

Lemma IV.2 Consider system (8) with hybrid feedback (3), (4), (7). Suppose automaton $\mathcal{A}_i(p_i,h)$, for some $i=1,2,3$, is not at state q_3^i, i.e., $q^i \in \{q_1^i, q_2^i\}$. There exists $\bar{\eta} \in (\delta,1)$ such that if state (q,ω) is such that $\eta \geq \bar{\eta}$, then $-\lambda_i(q,\omega_i,u_i^\star(q^i))$ in Lemma IV.1 is negative definite with respect to $(\epsilon_i,\omega_i)=(0,0)$.

The proofs of the foregoing lemmas are presented in the appendix. Lemma IV.1 establishes a bound on $\dot{V}^+$, while Lemma IV.2 states that there exists a neighborhood of equilibrium $(q,\omega)=(\mathbb{1},0)$ on which, as long as $u_i^\star(q^i) \in \{-1,1\}$ and $(\epsilon_i,\omega_i) \neq (0,0)$, $-\lambda_i(q,\omega_i,u_i^\star(q^i))$ in Lemma IV.1 will be negative definite.

Let U be an arbitrary open neighborhood of equilibrium $(q,\omega)=(\mathbb{1},0)$ in X. Pick $\delta \in (0,1)$ and define $X_{\bar{\eta}} := \{(q,\omega) \in X : \eta > \bar{\eta}\}$, with $\bar{\eta} \in (\delta,1)$ as in Lemma IV.2. For each real number $\rho>0$, denote $W_\rho := \{(q,\omega) \in X : \eta > 0,\ V^+(q,\omega) \leq \rho\}$. Let $\gamma_0>0$ be such that $W_{\gamma_0} \subset X_{\bar{\eta}}$ and let $\gamma_1 \in (0,\gamma_0)$ be such that $W_{\gamma_1} \subset U$. In the following it is shown that there exist controller parameters $p_i=(\delta_1^i,\delta_2^i,\kappa_i)$ in $\mathcal{A}_i(p_i,h)$, $i=1,2,3$, such that compact set $W_{\gamma_1} \subset U$ is made asymptotically stable for the closed loop system. This is proved by applying Theorem 7.8 in [18]. It must be shown that there exist controller parameters (p_1,p_2,p_3) in $\mathcal{A}_i$, $i=1,2,3$ such that the following holds

a) V^+ does not increase across state transitions of the automata $\mathcal{A}_i(p_i,h)$, $i=1,2,3$;

b) $\dot{V}^+ < 0$ on Int $W_{\gamma_0} \setminus W_{\gamma_1}$;

c) the closed-loop system does not admit Zeno solutions (i.e., any solution of the closed-loop system is characterized by an unbounded continuous time domain).

Let $\delta_2^i = \delta_2$, $i=1,2,3$, where $\delta_2>0$ is chosen such that $\{(q,\omega) \in X_{\bar{\eta}} : \|(\epsilon_i,\omega_i)\|_2 \leq \delta_2, \text{for all } i=1,2,3\} \subset \text{Int } W_{\gamma_1}$. Pick $\delta_1^i \in (0,\delta_2)$, $i=1,2,3$. By construction, if all the automata are at state q_3^i, $i=1,2,3$, then $(q,\omega) \in W_{\gamma_1}$. It is now verified that the conditions a) to c) hold.

Condition a) can be easily verified by noticing that V^+ is continuous across any state transitions of the automata.

Condition b) is now verified. The way parameter δ_2 was selected guarantees that, if $(q,\omega) \in$ Int $W_{\gamma_0} \setminus W_{\gamma_1}$, then at least one automaton is not in state q_3^i. In other words, for at least one $i=1,2,3$, $(\epsilon_i,\omega_i) \notin \bar{B}_{\delta_2}(0)$ and so $u_i^\star(q^i) \in \{-1,1\}$. Consider the following worst case scenario: suppose that two out of the three automata, say $\mathcal{A}_2$ and $\mathcal{A}_3$, are in state q_3^2 and q_3^3, respectively, with $(\epsilon_2,\omega_2),(\epsilon_3,\omega_3) \in \bar{B}_{\delta_2}(0)$ and $u_2^\star(q_3^2)=u_3^\star(q_3^3)=0$, while automaton $\mathcal{A}_1$ is either in state q_1^1 or q_2^1, i.e., $u_1^\star(q^1) \in \{-1,1\}$. By Lemma IV.1, $\dot{V}^+$ is upper-bounded by $-\lambda_1(q,\omega_1,u_1^\star(q^1)) - \lambda_2(q,\omega_2,0) - \lambda_3(q,\omega_3,0)$, with $-\lambda_i(q,\omega_i,u_i^\star(q^i))$, $i=1,2,3$, given by Lemma IV.1. Since the function $-\lambda_2(q,\omega_2,0) - \lambda_3(q,\omega_3,0)$ is continuous, since $(\epsilon_2,\omega_2),(\epsilon_3,\omega_3) \in \bar{B}_{\delta_2}(0)$, a compact set,

and since $q \in \mathbb{S}^3$, also a compact set, it follows that there exists a continuous, positive-definite function $w(\delta_2)$ such that $-\lambda_2(q,\omega_2,0) - \lambda_3(q,\omega_3,0) \leq w(\delta_2)$, which implies that

$$\dot{V}^+ \leq -\lambda_1(q,\omega_1,u_1^\star(q^1)) + w(\delta_2).$$

In the scenario considered here, on the set $W_{\gamma_0} \setminus W_{\gamma_1}$, the automaton $\mathcal{A}_1$ can only be at state $q^1 \in \{q_1^1, q_2^1\}$. For each such q^1, Lemmas IV.1 and IV.2 guarantee that the function $(q,\omega_1) \mapsto \lambda_1(q,\omega_1,u_1^\star(q^1))$ is continuous and negative definite on W_{γ_0}, thus there exists $\bar{\lambda} > 0$ such that $-\lambda_1(q,\omega_1,u_1^\star(q^1)) \leq -\bar{\lambda}$ on Int $W_{\gamma_0} \setminus W_{\gamma_1}$. Since $w(\delta_2)$ is continuous and $w(0) = 0$, there exists $\delta_2^* > 0$ such that for all $\delta_2 \in (0,\delta_2^*)$, $w(\delta_2) < \bar{\lambda}$. Therefore, for all $\delta_2 \in (0,\delta_2^*)$ and all $(q,\omega) \in$ Int $W_{\gamma_0} \setminus W_{\gamma_1}$ with $(\epsilon_2,\omega_2),(\epsilon_3,\omega_3) \in \bar{B}_{\delta_2}(0)$, $\dot{V}^+ < 0$. The other scenarios (only one automaton in state q_3^i, or none at all) are handled in an analogous manner. This shows that $\dot{V}^+ < 0$ on Int $W_{\gamma_0} \setminus W_{\gamma_1}$.

Condition c) can be verified by showing that the number of state transitions performed by any automaton $\mathcal{H}(\delta)$ and $\mathcal{A}_i(p_i,h)$ is uniformly bounded over compact sets of initial conditions and over compact time intervals. Consider a compact set of initial conditions W_γ, with $\gamma \in [\gamma_0,\gamma_1)$ and let $\bar{\omega} = \max\{|\omega_i(0)|,2\}$, as $(q(0),\omega(0))$ varies over W_γ. It is easy to show that set $\mathbb{S}^3 \times \{\omega : |\omega_i| \leq \bar{\omega}\} \supset W_\gamma$ is positively invariant. Hence, for any initial condition in W_γ, $\|\omega\|_2$ is bounded from above. This implies that $|\dot{\omega}_i|, |\dot{\epsilon}_i|$, $i = 1,2,3$, and $|\dot{\eta}|$ are uniformly bounded as well. Since $|\dot{\eta}|$ is bounded, it immediately follows that the time between consecutive state transitions of automaton $\mathcal{H}(\delta)$ is bounded. Since $|\dot{\omega}_i|, |\dot{\epsilon}_i|$, $i = 1,2,3$, are uniformly bounded, it follows that the time between consecutive state transitions involving states q_1^i and q_2^i is lower bounded by a constant $T_1 > 0$, since $\xi_i = (\epsilon_i,\omega_i)$ must cover a minimum distance bounded from zero to trigger a state transition. Similarly, the time between two consecutive state transitions of the type $q_j^i \to q_3^i$, followed by $q_3^i \to q_k^i$, with $j,k \in \{1,2\}$ is lower bounded by a constant $T_2 > 0$. There are sequences of state transitions for which a lower non-zero bound does not exist. Similarly to what was shown in the proof of Theorem 1 in [8], these specific sequences are always followed by one of the sequences presented above. Hence, for any $T > 0$ there exists $N > 0$ such that for each initial condition in W_γ automaton $\mathcal{A}_i(p_i,h)$ undergoes at most N state transitions over any compact time interval of length T.

This proves that the proposed controller practically stabilizes the equilibrium $(q,\omega) = (\mathbb{1},0)$, with basin of attraction containing the set W_{γ_0}. A similar analysis can be repeated on a neighborhood of equilibrium $(q,\omega) = (-\mathbb{1},0)$ with Lyapunov function $V^- = V^+(-q,\omega)$, to prove that the controller practically stabilizes equilibrium $(q,\omega) = (-\mathbb{1},0)$. This concludes the proof of the theorem. □

V. Numerical Estimation of the Controller's Basin of Attraction

The results presented in Section IV show that the proposed controller solves the bang-bang attitude control problem locally. It is of crucial importance for engineering applications to provide an estimation of the controller's basin of attraction. This section presents a Monte Carlo numerical study aimed at convincing the reader that the convergence of the proposed controller might, in fact, be global, i.e., the controller's basin of attraction is the whole state space X. Throughout this section the non-dimensional system (8) with controller (3), (4), (7) is considered so as to eliminate any dependency on a specific choice for parameters J_0 and $\bar{\tau}$. In order to improve the accuracy of the simulation, the coordinate transformation has been modified so to have $u_i \in \{-0.1, 0, +0.1\}$ for all $i = 1,2,3$. This can be done by replacing any $\sqrt{J_0/\bar{\tau}}$ term with $\sqrt{J_0/(10\bar{\tau})}$.

To show that the convergence of the proposed controller is global a large set of initial conditions (several thousands) is picked randomly and it is shown that for any of the chosen initial conditions the proposed controller meets the control specifications.

A. Simulations Setup

Let $X_C := \mathbb{S}^3 \times \{(\omega_1, \omega_2, \omega_3) \in \mathbb{R}^3 : |\omega_i| \leq 2\sqrt{\bar{u}}\}$. One can easily show (the proof is omitted due to space limitations) that set X_C is globally attractive and positively invariant for the closed-loop system. Thanks to this fact, it is enough to pick initial conditions in set X_C to show that the proposed controller yields global convergence. After an initial condition is chosen, the controller is to be initialized. Particular care needs to be applied in performing this operation: any simulation initial condition (q_0, ω_0) can be seen as the actual initial conditions of the system or as the state of the spacecraft some time after it entered X_C, being initialized outside set X_C. This ambiguity in the interpretation of each simulation initial condition can lead to different initialization of automata $\mathcal{H}(\delta)$ and $\mathcal{A}_i(p_i, h)$. The following strategy is adopted: any time one of the automata could be initialized to multiple different states because of this issue, the automata is initialized randomly.

Control parameters p_i were selected the same for all the automata, i.e., $p_i = p = (\delta_1, \delta_2, \kappa)$, for all $i = 1, 2, 3$, with $\delta_1 = 1 \cdot 10^{-4}$, $\delta_2 = 5 \cdot 10^{-4}$ and $\kappa = 0$. Supervisor hysteresis parameter has been selected to $\delta = 0.04$.

Each simulation is stopped when all three automata are at state q_3^i, i.e., $u_i^\star(q_3^i) = 0$ and $(\epsilon_i, \omega_i) \in \bar{B}_{\delta_2}(0)$ for all i. If the controller successfully triggers the simulation's stop condition the initial condition under study is included into the basin of attraction of the controller. A total of 6000 simulations was performed.

Remark V.1 In practice one can pick $\delta_2^i = \delta_2 > 0$, for all $i = 1, 2, 3$, and choose the value of δ_2 knowing that the controller will steer the state (q, ω) into a neighborhood $U = \{(q, \omega) : |\eta| > \tilde{\eta},\ \|\omega\|_2 < \tilde{\omega}\}$ of $(q, \omega) = (\pm\mathbb{1}, 0)$, with $\tilde{\eta} \approx \sqrt{1 - 3(\delta_2)^2}$ and $\tilde{\omega} \approx 2\sqrt{3\bar{u}\delta_2}$. Parameters δ_1^i must be picked such that $\delta_1^i \in (0, \delta_2)$, for all $i = 1, 2, 3$. In practice, the numerical value of δ_1^i affects only the controller switching frequency in a neighborhood of $(\epsilon_i, \omega_i) = (0, 0)$. Parameter δ can be chosen arbitrarily small so as to reduce the size of the neighborhood on which the controller might induce unwinding, i.e., $\eta \in (-\delta, +\delta)$. Notice, however, that as δ decreases the controller becomes less robust with respect to sensor noise.

B. Controller Performance

The performance of the proposed controller is evaluated through two main sets of parameters. The first set of parameters is meant to provide an insight into the overall ability of the controller to meet the control specifications and to evaluate the controller's performance during the transient. Each simulation solution is uniformly sampled every $\Delta t = 0.001$. A sampling time is denoted by t_k, with $k \in \{0, 1, \dots N\}$, where N is the total number of samples in a simulation. The following performance measures are recorded:

- **Success Rate (SR)**: SR records the percentage of simulations in which the proposed controller successfully triggered the simulation stopping condition.
- **Root Mean Square of the angular velocity error (e_ω)**: $e_\omega = \sqrt{\frac{1}{N}\sum_{k=0}^{N} \|\omega(t_k)\|_2^2}$;
- **Root Mean Square of the principal angle error (e_ϕ)**: $e_\phi = \sqrt{\frac{1}{N}\sum_{k=0}^{N} |\phi(t_k)|^2}$ where $\phi(t_k)$ denotes the principal angle associated to the spacecraft attitude at time t_k;
- **Total number of state transitions in automaton** $\mathcal{H}(\delta)$;
- **Non-dimensional simulation time** T.

The second set of parameters is meant to provide an insight into the performance of the on-board thrusters. For each simulation, the following quantities are recorded

- **Number of switches of each control torque $\boldsymbol{\tau_i}$** (n_i).

– **Mean switching frequency of each control torque τ_i (f_i):** f_i is computed as the mean of the controller switching frequency at each time step t_k of the simulation, $f_i(t_k)$. $f_i(t_k)$ is computed as the number of switches performed by control torque τ_i in the time window $\Delta t_k = [t_k - \Delta, t_k + \Delta]$, with $\Delta = 0.5$ (dimensionless).

C. Results

The success rate obtained across the simulations has been SR = 1.0. Hence, for any initial condition tested in X_C, the controller has successfully steered each (ϵ_i, ω_i) to $\bar{B}_{\delta_2}(0)$. We believe that the large volume of simulations, combined with the randomness in the selection of initial conditions presents compelling evidence to the claim that the proposed controller solves the bang-bang attitude control problem globally. The mean, maximum and minimum of quantities e_ω, e_ϕ, T across all the simulations performed (T can be easily converted to seconds by multiplying it by scale factor $\sqrt{J_0/(10\bar{\tau})}$) are presented in Table 1. These results will be used as benchmark when analyzing the performance of the controller during the transient when external perturbations and measurement noise are considered.

Table 1: Mean, Max and Min of e_ω, e_ϕ, T across all the simulations performed.

	e_ω	e_ϕ, rad	T
Mean across all simulations	0.3205	3.3116	12.459
Max across all simulations	0.4679	6.2192	19.6507
Min across all simulations	0.09	0.0682	2.3834

In Table 2 the statistical analysis of the switching behavior induced by the controller is presented. In particular, we focus on the mean, maximum and minimum of the number of switches and of the controller switching frequency across all the simulations performed.

Table 2: Mean, Max and Min of n_i, f_i with $i \in \{1, 2, 3\}$ across all the simulations performed.

	n_1	n_2	n_3	f_1	f_2	f_3
Mean across all simulations	6	6	6	0.4736	0.4732	0.4733
Max across all simulations	48	34	39	3.31367	4.896	4.896
Min across all simulations	2	2	2	0.1447	0.1286	0.1286

Of particular interest is the analysis of the number of switches induced by the controller. One can see from Table 2 that the minimum number of switches performed per channel is 2 as in the case of the time-optimal controller for double-integrators. The maximum number of switches correspond to situations in which one of the initial conditions $(\epsilon_i(0), \omega_i(0))$ is initialized very close to the origin. In this case, (ϵ_i, ω_i) bounces between switching sets Λ_i^+ and Λ_i^- until the rest of the state has converged sufficiently close to the origin.

It is interesting to observe that only 8.88% of the simulations performed displayed a state transition in automaton $\mathcal{H}(\delta)$. Moreover, automaton $\mathcal{H}(\delta)$ never performed more than one single state transition. This seems to suggest that once $(q, \omega) \in X_C$, the anti-unwinding supervisor $\mathcal{H}(\delta)$ will switch the equilibrium to stabilize at most once.

In the following, the results for one of the simulations performed are presented so to provide a better understanding of the controller performance. The initial conditions were randomly chosen at $q(0) = (0.6556, -0.3414, -0.6686, -0.2901)$ and $\omega(0) = (0.5410, -0.0496, -0.0809)$ (ω in non dimensional). Since $\eta(0) < -\delta$, automaton $\mathcal{H}(\delta)$ is initialized at state $h = -1$. Automata $\mathcal{A}_i(p, -1)$ are then initialized according to the rules presented in (4), with $\xi_i = (-\epsilon_i, \omega_i)$. In this case, the set of initials states of the automata $\mathcal{A}_i(p, -1)$ is $\{q_2^1, q_1^2, q_1^3\}$, which implies that $u^\star = (+\bar{u}, -\bar{u}, -\bar{u})$.

The trajectories of states (ϵ_i, ω_i), with $i = 1, 2, 3$, are shown in Figures 4 to 6. It is immediate to notice that the proposed controller steers each (ϵ_i, ω_i) to a neighborhood of $(\epsilon_i, \omega_i) = (0, 0)$. Figure 7 clearly shows that the controller steers the spacecraft state (q, ω) to a neighborhood of $(\mathbb{1}, 0)$, in that $\eta(t)$ is steered towards $+1$. Automaton $\mathcal{H}(\delta)$ undergoes a single state transition $-1 \to +1$ to prevent the insurgence of unwinding. As shown in Figure 7, η overshoots past the threshold $\eta \geq \delta$, triggering the state transition $-1 \to +1$ in automaton $\mathcal{H}(\delta)$. After the transition, the low-level controller stabilizes what is now the "closest" equilibrium in X, i.e., $(\mathbb{1}, 0)$, instead of forcing the state back to $(-\mathbb{1}, 0)$. This clearly shows how the action of supervisor $\mathcal{H}(\delta)$ prevents the insurgence of unwinding in the closed loop dynamics. The state transition of $\mathcal{H}(\delta)$ is indicated in the figures by a star symbol.

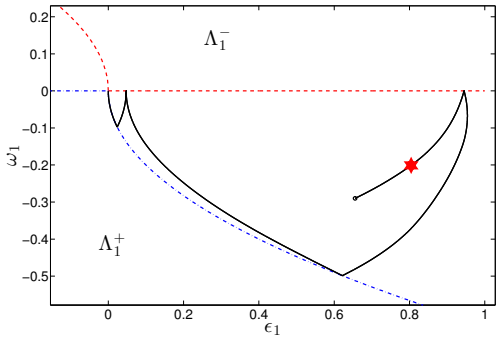

Fig. 4: Trajectory of $(\epsilon_1(t), \omega_1(t))$. The star identifies the transition $-1 \to +1$ in automaton $\mathcal{H}(\delta)$.

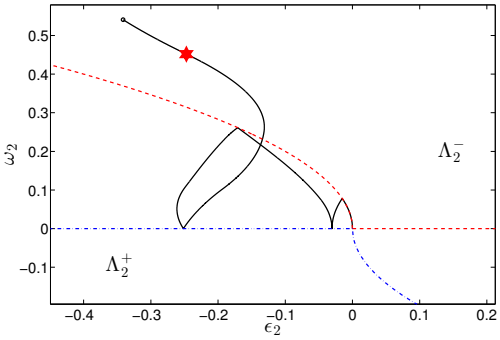

Fig. 5: Trajectory of $(\epsilon_2(t), \omega_2(t))$. The star identifies the transition $-1 \to +1$ in automaton $\mathcal{H}(\delta)$.

Figure 8 shows the switching history of the three control inputs on-off state u_i. Clearly, the proposed controller successfully avoids the generation of high-frequency switching behaviors.

VI. Robustness with Respect to Measurement Noise

This section presents a Monte Carlo numerical investigation of the robustness properties of the proposed controller against measurement noise. Let $(\hat{q}, \hat{\omega})$ denote the measured state. When measurement noise is considered, automata $\mathcal{H}(\delta)$ and $\mathcal{A}_i(p_i, h)$, with $i = 1, 2, 3$, undergo state transitions when the measured states $\hat{\eta}$ and $\hat{\xi}_i = (h\hat{\epsilon}_i, \hat{\omega}_i)$ satisfy the state transition conditions, instead of η and $\xi_i = (h\epsilon_i, \omega_i)$. The quaternion measurements $\hat{q}$ are generated as follows (see [19], [20])

$$\hat{q} = (\tilde{q} \oplus q)/\|\tilde{q} \oplus q\|$$

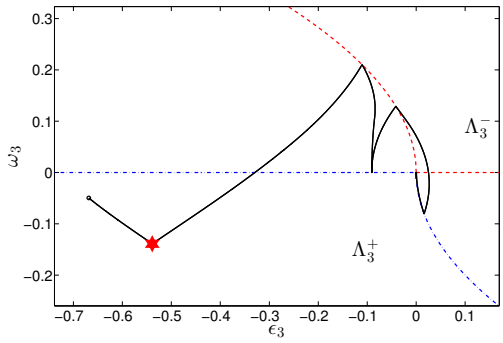

Fig. 6: Trajectory of $(\epsilon_3(t), \omega_3(t))$. The star identifies the transition $-1 \to +1$ in automaton $\mathcal{H}(\delta)$. Notice how in this case a switch in the control input value is triggered as $\mathcal{H}(\delta)$ switches value of parameter h. As h is set to $+1$, $\xi_3 = (\epsilon_3, \omega_3)$ immediately meets the transition condition that triggers the jump $q_1^3 \to q_2^3$.

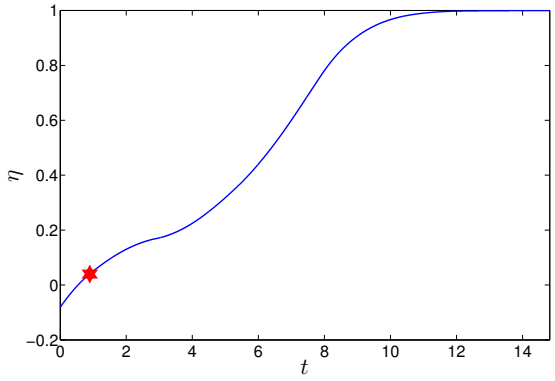

Fig. 7: Time history of state η. The red star identifies the transition $-1 \to +1$ in automaton $\mathcal{H}(\delta)$. If the action of the supervisor is prevented, the proposed controller would force the state back towards $(-\mathbb{1}, 0)$, generating unwinding.

where $[\tilde{q} \oplus]$ is defined as

$$[\tilde{q} \oplus] = \begin{bmatrix} \tilde{\eta} & \tilde{\epsilon}_3 & -\tilde{\epsilon}_2 & \tilde{\epsilon}_1 \\ -\tilde{\epsilon}_3 & \tilde{\eta} & \tilde{\epsilon}_1 & \tilde{\epsilon}_2 \\ \tilde{\epsilon}_2 & -\tilde{\epsilon}_1 & \tilde{\eta} & \tilde{\epsilon}_3 \\ -\tilde{\epsilon}_1 & -\tilde{\epsilon}_2 & -\tilde{\epsilon}_3 & \tilde{\eta} \end{bmatrix}.$$

Vector $\tilde{q}$ is generated as $\tilde{q} = (1/2\delta q, +1)$ where $\delta q \in \mathbb{R}^3$ is sampled from a zero-mean Gaussian distribution with covariance $\sigma_q^2 = (0.001)\ I\ \text{deg}^2$.
The angular velocity measurements are generated as $\hat{\omega} = \omega + \delta\omega$ where $\delta\omega \in \mathbb{R}^3$ is sampled from a zero-mean Gaussian distribution with covariance $\sigma_\omega^2 = (9 \cdot 10^{-8})\ I$ (ω is non-dimensional). Parameters δ_1 and δ_2 were taken with values $\delta_1 = 1 \cdot 10^{-3}$ and $\delta_2 = 3 \cdot 10^{-3}$. In this case, particular care must be adopted in choosing parameters δ_1, δ_2 so to avoid the insurgence of high-frequency switching at the origin. An in-depth analysis of this issue can be found in [8]. A total of 6000 simulations was performed, obtaining a success rate of SR = 1.0. The results of the numerical study are summarized in Table 3 and 4.

It can be seen from Table 3 that the performances indices characterizing the closed-loop behavior of the system during the transient are comparable to the nominal performances presented in Table

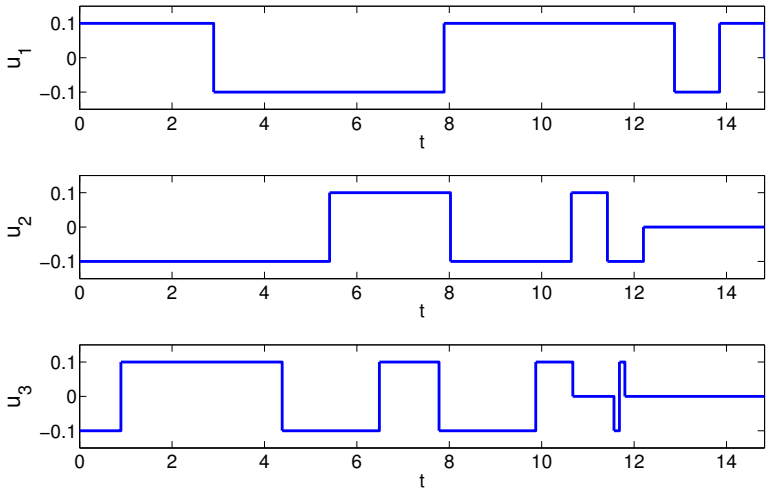

Fig. 8: Controller switching history.

Table 3: Mean, Max and Min of e_ω, e_ϕ, T across all the simulations performed.

	e_ω	e_ϕ, rad	T
Mean across all simulations	0.3202	3.3166	12.4208
Max across all simulations	0.4677	6.1878	20.7325
Min across all simulations	0.0603	0.0246	1.6827

Table 4: Mean, Max and Min of n_i, f_i with $i = 1, 2, 3$ across all the simulations performed.

	n_1	n_2	n_3	f_1	f_2	f_3
Mean across all simulations	5.2630	5.4278	5.3617	0.4111	0.4241	0.4240
Max across all simulations	31	30	34	2.6013	2.4305	2.4305
Min across all simulations	1	2	1	0.0859	0.1198	0.1198

1. This suggests that that the performance degradation induced by the presence of measurement noise is minimal. The number of switches and the switching frequency (see Table 4) also remain comparable to the nominal case (see Table 2). The decrease in the mean number of required switches to meet the control specifications is easily explained by the fact that the values for parameter δ_1 and δ_2 were chosen larger than in the nominal case. Notice that in this case the minimum number of switches for channels one and three is only 1: this corresponds to cases in which one of the (ϵ_i, ω_i) enters $\bar{B}_{\delta_1}(0)$ directly without ever entering any of the switching sets Λ_i^+, Λ_i^-.

VII. Robustness with Respect to External Perturbations

In this section a numerical analysis is proposed that investigates the robustness of the proposed controller with respect to external bounded perturbations. Following a similar approach to the one outlined in Section IV, one can prove that the proposed controller locally solves the bang-bang attitude control problem even under the effects of small external perturbations (we omit the proof due to space limitations). Since the proposed analysis is local, this result can also be applied to show that the proposed controller solves the bang-bang attitude control problem for inertially asymmetric rigid bodies.

This section investigates the performances of the proposed controller when applied to an asymmetric rigid spacecraft perturbed by gravity-gradient torques. Consider the system

$$\begin{aligned} \dot{\epsilon} &= \tfrac{1}{2}\left(\eta I + S(\epsilon)\right)\Omega \\ \dot{\eta} &= -\tfrac{1}{2}\epsilon^T\Omega \\ J\dot{\Omega} &= S(J\Omega)\Omega + \tau + \tau_g, \end{aligned} \tag{11}$$

with $J = \text{diag}(100, 120, 140)$ kg $\cdot$ m^2 and $\bar{\tau}_i = 1$ N $\cdot$ m for all i. Control parameters $\bar{u}_i = \bar{\tau}_i/J_i$ are then given by the triple $(\bar{u}_1, \bar{u}_2, \bar{u}_3) = (0.01, 0.0083, 0.0071)1/\text{s}^2$. Torque τ_g denotes the gravity-gradient torque perturbing the spacecraft rotational dynamics. The spacecraft is assumed to be flying along a LEO circular orbit of radius $R_c = 6671$ km, inclination of $\pi/6$ radians, longitude of the ascending node of $\pi/3$ radians and argument of perigee of $\pi/4$ radians. Let $n = \sqrt{\mu/R_c^3}$, where $\mu = 3.98 \cdot 10^{14}$ m^3/s^2 is the Earth standard gravitational constant. The gravity gradient torque $\tau_g \in \mathbb{R}^3$ is given by

$$\tau_g = 3n^2 \left(\frac{r_s}{\|r_s\|}\right) \times \left(J\frac{r_s}{\|r_s\|}\right),$$

where r_s is the position vector of the spacecraft with respect to Earth written in frame $\mathcal{B}$. As done in Section V, the simulations' initial conditions are picked from set $\mathbb{S}^3 \times \{(\Omega_1, \Omega_2, \Omega_3) \in \mathbb{R}^3 : \Omega_i \in [-2\sqrt{\bar{u}_i}, +2\sqrt{\bar{u}_i}]\}$ (however, in this case, the set is no longer positively invariant and globally attractive). The performance of the controller has been tested as the spacecraft moves along the orbit. In particular 100 simulations were performed every $\pi/6$ radians along the orbit, for a total of 1200 simulations. Parameters δ_1, δ_2 were chosen as $\delta_1 = 2 \cdot 10^{-4}$ and $\delta_2 = 6 \cdot 10^{-4}$. The success rate over the set of simulations was SR = 1.0. The results are summarized using the performance metrics introduced in the Section V.

Table 5: Mean, Max and Min of e_ω, e_ϕ, T across all the simulations performed.

	e_ω, rad/s	e_ϕ, rad	T, s
Mean across all simulations	0.0932	3.3055	44.1678
Max across all simulations	0.1344	6.1708	69.2408
Min across all simulations	0.0241	0.0740	8.6581

The results in Table 5 can be compared to the nominal performance of the controller presented in Table 1 by using the scaling factor $\sqrt{J_2/(10\bar{\tau})} = 3.4641$ s. This corresponds to scaling the results so to provide an estimate of the performance of the proposed controller when controlling a symmetric spacecraft with $\bar{\tau} = 1$ N $\cdot$ m and $J_0 = J_2 = 120$ kg $\cdot$ m^2. This gives us the opportunity to evaluate the effects of external perturbations and asymmetries of the spacecraft on the controller performance during the transient. Notice, however, that in the two simulations different values of δ_1 and δ_2 were used. Moreover, the sampling time used to sample the solutions is changed by the scaling factor $\sqrt{J_2/(10\bar{\tau})}$. The results are presented in Table 6.

Table 6: Mean, Max and Min of e_ω, e_ϕ, T across all the simulations performed for a symmetric spacecraft with $\bar{\tau} = 1$ N $\cdot$ m and $J_0 = 120$ kg $\cdot$ m^2.

	e_ω, rad/s	e_ϕ, rad	T, s
Mean across all simulations	0.0925	3.3116	43.1592
Max across all simulations	0.1351	6.2192	68.072
Min across all simulations	0.026	0.0682	8.2563

The data in Table 5 and 6 clearly show that the performance of the proposed controller remain very close to the nominal performances when small external perturbations and asymmetries are considered.

Table 7: Mean, Max and Min of $n_i,\ f_i$ with $i = 1, 2, 3$ across all the simulations performed.

	n_1	n_2	n_3	$f_1,\ 1/\text{s}$	$f_2,\ 1/\text{s}$	$f_3,\ 1/\text{s}$
Mean across all simulations	8.4308	7.2208	5.9017	0.1879	0.1641	0.164
Max across all simulations	43	66	31	1.1997	1.8128	1.8128
Min across all simulations	2	2	2	0.0422	0.0422	0.0932

The results summarized in Table 7 show how, even in the worst scenarios, the required thrusters switching frequency is easily achievable given the state of today's technology. It is also interesting to notice how, on average, $n_1 > n_2 > n_3$. This can be easily explained by noticing that since $J_1 < J_2 < J_3$, then $\bar{u}_1 > \bar{u}_2 > \bar{u}_3$. Hence, the closed-loop dynamics along the first axis tends to be *faster* than the dynamics along the other axes. On average then, (ϵ_1, ω_1) will converge to the origin faster the the other states. Automaton $\mathcal{A}_1(p, h)$ will then be forced to turn on and off the associated control torque a few times before the simulation's stop condition is triggered. This also explains the fact that in this case more control switches are required then in the nominal case presented in Table 1.

VIII. Conclusions

The paper presents a novel hybrid bang-bang controller that solves the bang-bang attitude control problem. The proposed controller successfully stabilizes any desired spacecraft attitude without inducing high-frequency switching of the actuators. Extensive simulation analysis suggests that the proposed controller may in fact yield global practical stability of the target spacecraft attitude. It was also verified that the proposed controller solves the bang-bang attitude control problem irrespective of external perturbations and measurement noise.

Appendix: Proofs of Lemma IV.1 and Lemma IV.2

Proof of Lemma IV.1 Let $V_\epsilon^+ = \partial V^+/\partial \epsilon =: [V_{\epsilon_1}^+\ V_{\epsilon_2}^+\ V_{\epsilon_3}^+]$, $V_\omega^+ = \partial V^+/\partial \omega =: [V_{\omega_1}^+\ V_{\omega_2}^+\ V_{\omega_3}^+]$ where

$$\begin{aligned} V_{\epsilon_i}^+ = \partial V^+/\partial \epsilon_i =& 8\epsilon_i\omega_i\sigma(\epsilon_i,\omega_i) + \frac{4}{3}\omega_i^3 + 4\sigma(\epsilon_i,\omega_i)\left(2\epsilon_i\sigma(\epsilon_i,\omega_i) + \frac{1}{2}\omega_i^2\right)^{\frac{3}{2}} \\ V_{\omega_i}^+ = \partial V^+/\partial \omega_i =& 4\epsilon_i^2\sigma(\epsilon_i,\omega_i) + 4\omega_i^2\epsilon + \frac{3}{4}\omega_i^4\sigma(\epsilon_i,\omega_i) + 2\omega_i\left(2\epsilon_i\sigma(\epsilon_i,\omega_i) + \frac{1}{2}\omega_i^2\right)^{\frac{3}{2}}. \end{aligned} \tag{12}$$

$\dot{V}^+$ is then given by

$$\dot{V}^+ = \frac{1}{2}V_\epsilon^+\left(\eta I + S(\epsilon)\right)\omega + V_\omega^+ u^\star(q^1, q^2, q^3),$$

with $u^\star(q^1, q^2, q^3) = (u_1^\star(q^1), u_2^\star(q^2), u_3^\star(q^3))$. By applying the Cauchy-Schwarz inequality we deduce an upper bound on $\dot{V}^+$ as

$$\dot{V}^+ \leq \sum_{i=1}^{3}\left(\frac{1}{2}\eta\omega_i V_{\epsilon_i}^+ + V_{\omega_i}^+ u_i^\star(q^i)\right) + \frac{1}{2}\|V_\epsilon^+\|_2\|S(\epsilon)\|_2\|\omega\|_2.$$

It is left to compute an upper bound for $1/2\|V_\epsilon^+\|_2\|S(\epsilon)\|_2\|\omega\|_2$. Let $(V_\epsilon^+)^\top$ be written as $(V_\epsilon^+)^\top = 8w + 4/3y + 4z$ where $w, y, z \in \mathbb{R}^3$ with $w_i = \epsilon_i\omega_i\sigma(\epsilon_i,\omega_i)$, $y_i = \omega_i^3$, $z_i = \sigma(\epsilon_i,\omega_i)\left(2\epsilon_i\sigma(\epsilon_i,\omega_i) + 1/2\,\omega_i^2\right)^{\frac{3}{2}}$, $i = 1, 2, 3$. Since $\|S(\epsilon)\|_2 = \sqrt{1-\eta^2}$, one can then write

$$\frac{1}{2}\|V_\epsilon^+\|_2\|S(\epsilon)\|_2\|\omega\|_2 \leq \frac{1}{2}\sqrt{1-\eta^2}\left(8\|w\|_2 + \frac{4}{3}\|y\|_2 + 4\|z\|_2\right)\|\omega\|_2. \tag{13}$$

First $\|w\|_2$ is computed. It is immediate to show that $\|w\|_2 \leq \|\epsilon\|_2\|\omega\|_2$. By applying Young's inequality one show that the first term of (13) is bounded by

$$4\sqrt{1-\eta^2}\|w\|_2\|\omega\|_2 \leq 2\sqrt{1-\eta^2}(\|\epsilon\|_2^2 + a^4\|\omega\|_4^4), \tag{14}$$

where $a > 0$ such that $\|\omega\|_2 \leq a\|\omega\|_4$ (all $p-$norms are equivalent in $\mathbb{R}^n$). A similar procedure can be followed to show that $\|y\|_2 \leq \|\omega\|_2^3$. The second term of the bound in (13) is given by

$$\frac{1}{2}\left(\frac{4}{3}\|y\|_2\right)\|S(\epsilon)\|_2\|\omega\|_2 \leq \frac{2}{3}a^4\sqrt{1-\eta^2}\|\omega\|_4^4. \tag{15}$$

Lastly, a bound on the last term of (13). It is immediate to show that

$$\|z\|_2 \leq \sqrt{\left(\sum_{i=1}^{3} 2|\epsilon_i| + \frac{1}{2}\omega_i^2\right)^3} \leq (2\|\epsilon\|_1 + \frac{1}{2}\|\omega\|_2^2)^{\frac{3}{2}}.$$

By using the fact that $(2\|\epsilon\|_1 + 1/2\ \|\omega\|_2^2)^{\frac{1}{2}} \leq \sqrt{2\|\epsilon\|_1} + 1/\sqrt{2}\ \|\omega\|_2$ and since there exists $b > 0$ such that $\|\epsilon\|_1 \leq b\|\epsilon\|_2$ one can write the last term of the bound in (13), after repeated applications of Young's inequality, as follows

$$\frac{1}{2}\left(2\|z\|_2\right)\|S(\epsilon)\|_2\|\omega\|_2 \leq 2\sqrt{1-\eta^2}\left(\hat{\alpha}\|\epsilon\|_2^2 + \hat{\beta}\|\omega\|_4^4\right), \tag{16}$$

for some $\hat{\alpha}, \hat{\beta} > 0$. Using the expressions in Eq. (14) to (16) one can write

$$\frac{1}{2}\|V_\epsilon^+\|_2\|S(\epsilon)\|_2\|\omega\|_2 < \alpha\sqrt{1-\eta^2}\|\epsilon\|_2^2 + \beta\sqrt{1-\eta^2}\|\omega\|_4^4,$$

where $\alpha = 2(1+\hat{\alpha})$ and $\beta = 8/3\ a^4 + 2\hat{\beta}$. It follows that

$$\dot{V}^+ \leq \sum_{i=1}^{3} -\lambda_i(q, \omega_i, u_i^\star(q^i)),$$

where $-\lambda_i(q, \omega_i, u_i^\star(q^i)) = 1/2\ \eta\omega_i V_{\epsilon_i}^+ + V_{\omega_i}^+ u_i^\star(q^i) + \alpha\sqrt{1-\eta^2}\epsilon_i^2 + \beta\sqrt{1-\eta^2}\omega_i^4$. This concludes the proof of the lemma. □

Proof of Lemma IV.2 Consider the case $\eta > \delta$, so that the supervisor output $h = +1$ is broadcasted to automata $\mathcal{A}_i(p_i, h)$, $i = 1, 2, 3$. Referring to Figure 9, define sets K_i^+ and K_i^-, with $i = 1, 2, 3$, as

$$K_i^+ = \{(\epsilon_i, \omega_i) : \epsilon_i \geq 0,\ -2\sqrt{\epsilon_i} \leq \omega_i \leq -2\sqrt{\kappa_i\epsilon_i}\} \tag{17}$$

$$K_i^- = \{(\epsilon_i, \omega_i) : \epsilon_i \leq 0,\ 2\sqrt{-\kappa_i\epsilon_i} \leq \omega_i \leq 2\sqrt{-\epsilon_i}\} \tag{18}$$

where $\kappa_i \in [0, +1)$ is the same parameter used in Section III to design the switching sets Λ_i^+, Λ_i^-.

Assume automaton $\mathcal{A}_i(p_i, +1)$, is not in state q_3^i, i.e. $u_i^\star(q^i) \in \{-1, +1\}$. Since then $\xi_i = (\epsilon_i, \omega_i)$, automaton $\mathcal{A}_i(p_i, +1)$ can the generate the following non-zero control inputs:

1. $u_i^\star(q^i) = -\sigma(\epsilon_i, \omega_i)$ can be generated for any (ϵ_i, ω_i);
2. $u_i^\star(q^i) = +\sigma(\epsilon_i, \omega_i)$ can be generated only if $(\epsilon_i, \omega_i) \in (K_i^+ \cup K_i^-)$.

Case 1 is studied first, i.e. it is assumed that $u_i^\star(q^i) = -\sigma(\epsilon_i, \omega_i)$. By applying the results presented in [21], one can show that

$$\frac{1}{2}\eta V_{\epsilon_i}^+\omega_i - V_{\omega_i}^+\sigma(\epsilon_i, \omega_i) = -\eta(4\epsilon_i^2 + \frac{1}{12}\omega_i^4) - (1-\eta)|V_{\omega_i}^+|.$$

Since $-(1-\eta)|V_{\omega_i}^+| \leq 0$, then $\lambda_i(q, \omega_i, -\sigma(\epsilon_i, \omega_i)) \leq -\eta(4\epsilon_i^2 + \frac{1}{12}\omega_i^4) + \alpha\sqrt{1-\eta^2}\epsilon_i^2 + \beta\sqrt{1-\eta^2}\omega_i^4$. It is immediate to see that there exists $\bar{\eta} \in (0, +1)$ such that for all $\eta \in [\bar{\eta}, +1]$, both $-4\eta + \alpha\sqrt{1-\eta^2} < 0$

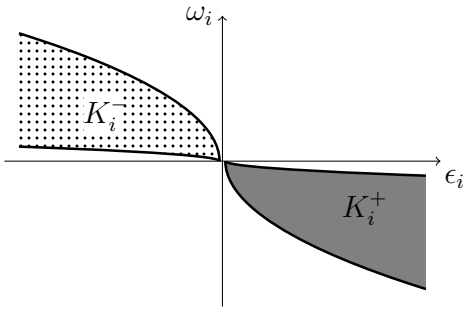

Fig. 9: Sets K_i^+ and K_i^- with $\kappa_i \in [0, 1)$.

and $-1/12\eta + \beta\sqrt{1-\eta^2} < 0$. It follows that if $\eta \geq \bar{\eta}$ then $\lambda_i(q, \omega_i, -\sigma(\epsilon_i, \omega_i)) < 0$ for all $(\epsilon_i, \omega_i) \neq (0, 0)$.

Consider case 2., i.e., $u_i^\star(q^i) = +\sigma(\epsilon_i, \omega_i)$ and $(\epsilon_i, \omega_i) \in (K_i^+ \cup K_i^-)$. It is immediate to verify that if $(\epsilon_i, \omega_i) \in (K_i^+ \cup K_i^-)$ then $\sigma(\epsilon_i, \omega_i)\epsilon_i = |\epsilon_i|$ and $\sigma(\epsilon_i, \omega_i)\omega_i = -|\omega_i|$. Using this fact one obtains that

$$\begin{aligned} \tfrac{1}{2}\eta V_{\epsilon_i}^+ \omega_i + V_{\omega_i}^+ \sigma(\epsilon_i, \omega_i) = \; & 4(1+\eta)\omega_i^2|\epsilon_i| + 4\epsilon_i^2 + \left(\tfrac{3}{4} + \tfrac{2}{3}\eta\right)\omega_i^4 - \\ & 2(1+\eta)|\omega_i|(2|\epsilon_i| + \tfrac{1}{2}\omega_i^2)^{\frac{3}{2}}. \end{aligned} \tag{19}$$

It can be shown that if $(\epsilon_i, \omega_i) \in (K_i^+ \cup K_i^-)$ then $|\omega_i|(2|\epsilon_i| + 1/2\omega_i^2)^{\frac{3}{2}} \geq \omega_i^2(2|\epsilon_i| + 1/2\omega_i^2)$. Using this fact in Eq. (19) allows us to conclude that

$$\frac{1}{2}\eta V_{\epsilon_i}^+ \omega_i + V_{\omega_i}^+ \sigma(\epsilon_i, \omega_i) \leq 4\epsilon_i^2 - \left(\frac{1}{3}\eta + \frac{1}{4}\right)\omega_i^4. \tag{20}$$

Substituting Eq. (20) in the expression for $\lambda_i(q, \omega_i, \sigma(\epsilon_i, \omega_i))$ implies that $\lambda_i(q, \omega_i, \sigma(\epsilon_i, \omega_i)) \leq \left(\alpha\sqrt{1-\eta^2} + 4\right)\epsilon_i^2 + \left(\beta\sqrt{1-\eta^2} - 1/3\eta - 1/4\right)\omega_i^4$. If $(\epsilon_i, \omega_i) \in (K_i^+ \cup K_i^-)$ then $|\omega_i|$ is bounded by $2\sqrt{\kappa_i|\epsilon_i|} \leq |\omega_i| \leq 2\sqrt{|\epsilon_i|}$. It follows that $\lambda_i(q, \omega, \sigma(\epsilon_i, \omega_i)) \leq g(\eta)\epsilon_i^2$, where $g(\eta) = \left(\alpha\sqrt{1-\eta^2} + 4 + 16\beta\sqrt{1-\eta^2} - (1/3\eta + 1/4)\,16\kappa_i^2\right)$. It is immediate to see that there exists $\bar{\kappa}_i < 1$ such that for all $\kappa_i \in (\bar{\kappa}_i, +1)$, $g(\eta = +1) < 0$. By continuity of $g(\eta)$, there exists $\bar{\eta} < 1$ such that $g(\eta) < 0$ for all $\eta \in [\bar{\eta}, +1]$. It follows that if $\eta \geq \bar{\eta}$, then $\lambda_i(q, \omega_i, \sigma(\epsilon_i, \omega_i)) \leq 0$ and $\lambda_i(q, \omega_i, \sigma(\epsilon_i, \omega_i)) = 0$ if and only if $\epsilon_i = 0$. Notice that since we are considering the case $(\epsilon_i, \omega_i) \in (K_i^+ \cup K_i^-)$, $\epsilon_i = 0$ if and only if $\omega_i = 0$ as well.

This concludes the proof of the lemma. □

References

[1] Silva, N., Martel, F., and Delpy, P., "Automated Transfer Vehicle Thrusters Selection and Management Function," 6th International ESA Conference on Guidance, Navigation and Control Systems, 2005.

[2] Souza, C. D., Hannak, C., Spehar, P., Clark, F., and Jackson, M., "Orion Rendezvous, Proximity Operations and Docking Design and Analysis," AIAA Guidance, Navigation and Control Conference and Exhibit, 2007.
doi:10.2514/6.2007-6683

[3] Agrawal, B. N. and Bang, H., "Robust Closed-Loop Control Design for Spacecraft Slew Maneuver Using Thrusters," *Journal of Guidance, Control, and Dynamics*, Vol. 18, No. 6, 1995, pp. 1336-1344.
doi:10.2514/3.21550

[4] Burdick, G. M., Lin, H.-S., and Wong, E. C., "A Scheme for Target Tracking and Pointing During Small Celestial Body Encounters," *Journal of Guidance, Control, and Dynamics*, Vol. 7, No. 4, 1984, pp. 450-457.
doi:10.2514/3.19877

[5] Agrawal, B. N., McClelland, R. S. and Song, G., "Attitude Control of Flexible Spacecraft Using Pulse-Width Pulse-Frequency Modulated Thrusters," *Space Technology*, Vol. 17, No. 1, 1997.
doi:10.1080/00207178408933308

[6] Wie, B., "Space Vehicle Dynamics and Control," Second Edition, AIAA, 2008.
doi:10.2514/4.860119

[7] Serpelloni, E., Maggiore, M. and Damaren, C. J., "A Bang-Bang Attitude Stabilizer for Rotating Rigid Bodies," Scitech 2016, San Diego, CA, USA.
doi:10.2514/6.2016-0368

[8] Serpelloni, E., Maggiore, M. and Damaren, C. J., "Bang-Bang Hybrid Stabilization of Perturbed Double-Integrators," *Automatica*, Vol. 69, 2016.
doi:10.1016/j.automatica.2016.02.028

[9] Bilimoria, K. D., and Wie, B., "Time-Optimal Three-Axis Reorientation of a Rigid Spacecraft," *Journal of Guidance, Control, and Dynamics*, Vol. 16, No. 3 (1993), pp. 446-452.
doi:10.2514/3.21030

[10] Byers, R. M. and Vadali, S. R., "Quasi-Closed-Form Solution to the Time-Optimal Rigid Spacecraft Reorientation Problem," *Journal of Guidance, Control, and Dynamics*, Vol. 16, No. 3, 1993, pp. 453-461.
doi:10.2514/3.21031

[11] Bai, X. and Junkins, J. L., "New Results for Time-Optimal Three-Axis Reorientation of a Rigid Spacecraft," *Journal of Guidance, Control, and Dynamics*, Vol. 32, No. 4, 2009, pp. 1071-1076.
doi:10.2514/1.43097

[12] Shen, H. and Tsiotras, P., "Time-Optimal Control of Axisymmetric Rigid Spacecraft Using Two Controls," *Journal of Guidance, Control, and Dynamics*, Vol. 22, No. 5, 1999, pp. 682-694.
doi:10.2514/2.4436

[13] Krishnan, H., Reyhanoglu, M., and McClamroch, H., "Attitude Stabilization of a Rigid Spacecraft Using Two Control Torques: A Nonlinear Control Approach Based on the Spacecraft Attitude Dynamics," *Automatica*, Vol. 30, No. 6, 1994, pp. 1023-1027.
doi:10.1016/0005-1098(94)90196-1

[14] Singh, S. and Iyer, A., "Nonlinear Decoupling Sliding Mode Control and Attitude Control of Spacecraft," *IEEE Transactions on Aerospace and Electronic Systems*, Vol. 25, No. 5, 1989, pp. 621-633.
doi:10.1109/7.42079

[15] Mayhew, C. G., Sanfelice, R. G., and Teel A. R., "Quaternion-Based Hybrid Control for Robust Global Attitude Tracking," *IEEE Transaction on Automatic Control*, Vol. 56, No. 11, 2011.
doi:10.1109/tac.2011.2108490

[16] Mayhew, C. G., Sanfelice, R. G., and Teel A. R., "On Path-Lifting Mechanisms and Unwinding in Quaternion-Based Attitude Control," *IEEE Transaction on Automatic Control*, Vol. 58, No. 5, 2013.
doi:10.1109/tac.2012.2235731

[17] Serpelloni, E., Maggiore, M., and Damaren, C. J., "Control of Spacecraft Formations Around the Libration Points Using Electric Motors with One Bit of Resolution," *Journal of the Astronautical Sciences*, Vol 61, No. 4, 2014.
doi:10.1007/s40295-014-0030-0

[18] Sanfelice, R. G., Goebel, R., and Teel, A. R., "Invariance Principles for Hybrid Systems With Connections to Detectability and Asymptotic Stability," *IEEE Transaction on Automatic Control*, Vol. 52, No. 12, 2007.
doi:10.1109/tac.2007.910684

[19] Crassidis, J., and Junkins, J., "*Optimal Estimation of Dynamic Systems*", Chapman and Hall/CRC, 2004.
doi:10.1201/9780203509128

[20] Barfoot, T., Forbes, J. R., and Furgale, P. T., "Pose Estimation Using Linearized Rotations and Quaternion Algebra," *Acta Astronautica*, Vol. 68, No. 1-2, 2010.
doi:10.1016/j.actaastro.2010.06.049

[21] Ryan, E. P., "Finite-Time Stabilization of Uncertain Nonlinear Planar Systems," *Dynamics and Control*, Vol. 1, No. 1, 1991.
doi:10.1007/bf02169426

[22] Goebel, R., Sanfelice, R. G., and Teel, A. R., "Hybrid Dynamical Systems," *IEEE Control Systems Magazine*, Vol. 29, No. 2, 2009.
doi:10.1109/mcs.2008.931718